

Virtual force node deployment algorithm of field observation instrument based on voronoi diagram

HUO Jiuyuan^{1,2,3*}, WANG Lei¹

1. School of Electronics and Information Engineering, Lanzhou Jiaotong University, Lanzhou 730070, China;

2. Lanzhou Huahao Technology co. Ltd., Lanzhou 730070, China;

3. National Cryosphere Desert Data Center, Lanzhou 730070, China

*Corresponding author: HUO Jiuyuan (huojy@mail.lzjtu.cn)

Received: July 14, 2024

Revised: September 10, 2024

Accepted: September 18, 2024

Abstract: Aiming at node deployment in the monitoring area of the field observation instrument network in the cold and arid regions, we propose a virtual force algorithm based on Voronoi diagram (VFVD), which adopts probabilistic sensing model that is more in line with the actual situation. First, the Voronoi diagram is constructed in the monitoring area to determine the Thiessen polygon of each node. Then, the virtual force on each node is calculated, and the node update its position according to the direction and size of the total force, so as to achieve the purpose of improving the network coverage rate. The simulation results show that the proposed algorithm can effectively improve the coverage rate of the network, and also has a good effect on the coverage uniformity.

Key words: field observation instrument network; node deployment; Voronoi diagram; virtual force; network coverage rate

0 Introduction

The cold and arid areas cover a vast area, where the ecological environment is fragile and complex, but it is rich in oil, coal and other natural resources, which has an important strategic position^[1]. After more than 50 years of development, the field monitoring network system covering the main ecological environment areas in cold and arid areas has been formed in China. This network provides an important scientific basis for scientific research in cold and arid regions, and is an important part of science and technology infrastructure, as well as an important base for scientific data collection and experimental research. It has made great contributions to the construction of major projects and sustainable economic development in the cold and arid areas of China, and has become an indispensable and irreplaceable support platform for scientific research in the cold and arid areas^[2].

Coverage availability is a prerequisite for application activities in wireless networks, and the deployment location of nodes has an important impact on network performance. According to the deployment method, node deployment is divided into deterministic

deployment and random deployment^[3]. In wireless sensor networks, the nodes are usually deployed in random deployment method. In order to improve the coverage of the monitoring area, a large number of sensor nodes are deployed, which leads to serious data redundancy in the network. Compared with sensor nodes, the number of instrument networking nodes is smaller and the cost is higher, so a deterministic deployment method is required. However, there is no mature node deployment algorithm for field observation instrument networking at present, so node deployment methods in wireless sensor network are used for node deployment, such as virtual force algorithm (VFA) algorithm, Voronoi diagram method, swarm intelligence optimization algorithm, etc.

Zou et al.^[4] used the VFA to optimize the deployment of nodes by calculating the virtual force between nodes to guide the nodes to the optimal position, so as to improve the coverage rate of the network. Considering the boolean sensing model and probabilistic sensing model respectively, Teng et al.^[5] proposed the virtual force algorithm based on density (IVFAB), which introduces the concept of node density into the VFA to determine the optimal distance threshold in the virtual force model, so as to optimize the deployment of nodes.

Li et al.^[6] proposed an optimized node deployment algorithm based on virtual force (WVFA). The algorithm achieves seamless coverage inside the coverage area by minimizing the redundant coverage area of nodes at the edge of the area, so as to optimizing node deployment. Zhou et al.^[7] proposed an improved virtual force relocation coverage enhancement algorithm (DV). The algorithm is divided into two stages. In the first stage, the Voronoi diagram is constructed to determine the uncovered area in each polygon and provide virtual force to the nodes to update its position. In the second stage, the Delaunay triangulation network is used to detect the coverage holes between sensors and repair them. Mahboubi et al.^[8] proposed two novel virtual force deployment algorithms. Firstly, the Voronoi diagram in the monitoring area is constructed. Then, the virtual force on the node is provided by the vertices and edges of the polygon where the node is located, which improves the oscillation phenomenon of the virtual force algorithm, and hence the network coverage rate is improved.

Fang et al.^[9] proposed a coverage control deployment strategy based on Thiessen's blind zone polygon centroid (BCBS). By areconstructing a Voronoi diagram in the monitoring area, the Thiessen polygon of each node is determined. After that, the blind area polygon inside the Thiessen polygon is got. Finally, the centroid of the blind area polygon is taken as expected target position of the node. Tan et al.^[10] proposed a three-dimensional spatial sensor node overlay algorithm based on weighted Voronoi diagram (TDWVADA). When the algorithm is running, the 3D weighted Voronoi diagram is constructed based on the position and weight of all nodes in the network, and then each sensor node is moved to the optimal deployment position, so as to improve the network coverage. Experimental results show that this algorithm can improve the network coverage of monitoring area more effectively.

Swarm intelligence optimization algorithm is developed by simulating the intelligent behavior of biological groups in nature, and they are widely favored by scholars for their flexibility and robustness in node deployment optimization. Ding et al.^[11] proposed a node deployment strategy based on improved particle swarm optimization (PSO) algorithm, which converts the area coverage problem into an optimization problem based on the set of feature points, To solve the problem that PSO algorithm is easy to fall into precocious state, the interference terms of inertia weights and local enhancement factors are proposed. Jin et al.^[12] proposed a node deployment algorithm based on genetic algorithm,

which aims to obtain higher coverage with a small number of nodes. The algorithm takes the overall network coverage and node connectivity as constraints, constructs an integer nonlinear programming model, and introduces a genetic algorithm to solve the optimal node deployment scheme. Jia et al.^[13] used genetic algorithms to optimize node deployment. The genetic algorithm has a strong global search capability, but its implementation is more complex and convergence is slow. Since the algorithm relies on the initial distribution of nodes, the stability of the algorithm is poor.

A good node deployment algorithm should make the nodes evenly distributed in the network, and the algorithm should have good global search capability to avoid uneven distribution of nodes in the monitoring area. The traditional virtual force algorithm views the nodes as charged particles, which are subject to interacting gravitational and repulsive forces, while the particles are also subject to boundary forces. The position of the particles is updated by the total force. However, the local nature of the force balance of the nodes can lead the algorithm to fall into a local optimum. Relying solely on the centroid of Thiessen polygon to guide the movement of the node can optimize the coverage of the polygon where the node is located, but it cannot provide stable and effective deployment in the whole network. Therefore, in order to improve the global search capability of the algorithm, we propose a virtual force algorithm method based on Voronoi diagram (VFAVD) for node deployment. The algorithm adopts a probabilistic sensing model. After constructing a Voronoi diagram in the monitoring area to determine the Thiessen polygon of each node, the virtual force applied to each node is calculated and the position of the node according to the direction and magnitude of total force is updated, thus achieving the objective of improving the network coverage.

1 Problem description

Assuming that the monitoring area is a two-dimensional planar area of $L \times L$ (unit: $m \times m$), N nodes need to be arranged in the monitoring area to maximize the coverage in the monitoring area. All nodes are homogeneous nodes with the same transmission radius and sensing radius, and the position of each node is noted as $S_i = (X_i, Y_i)$. Dividing the monitoring area into $L \times L$ squares with an area of $1 m^2$, and then simplifying the squares into pixels, the distance $d_{i,p}$ between the node S_i and the target pixel $p = (X_p, Y_p)$ can be calculated as

$$d_{i,p} = \sqrt{(X_i - X_p)^2 + (Y_i - Y_p)^2}. \quad (1)$$

The instrument node adopts the probability sensing model^[14]. Compared with the boolean sensing model, the probability sensing model is more suitable for the actual situation of nodes. As shown in Fig. 1, the innermost solid circle is the certain area, the area between the solid circle and the outermost dashed line is the uncertain area, and the area outside the outermost dashed line is the unobservable area. The probability $C_{p,i}$ that pixels p can be monitored by node S_i is shown as

$$C_{p,i} = \begin{cases} 0, & d_{i,p} \geq R_s + r_e, \\ e^{(-\lambda_1 \alpha_1^{\beta_1} / \alpha_2^{\beta_2} + \lambda_2)}, & R_s - r_e < d_{i,p} < R_s + r_e, \\ 1, & d_{i,p} \leq R_s - r_e, \end{cases} \quad (2)$$

where $d_{i,p}$ represents the distance from point p to node S_i ; R_s is the sensing radius of node S_i ; r_e is the measurement reliability parameter of the node; $\alpha_1 = r_e - R_s + d_{i,p}$, $\alpha_2 = r_e + R_s - d_{i,p}$, $\alpha_1 > 0$, $\alpha_2 > 0$; λ_1 , λ_2 , β_1 , and β_2 are measurement parameters related to the characteristics of the node, $\lambda_1 = 1$, $\lambda_2 = 0$, $\beta_1 = 1$, $\beta_2 = 1.5$. Fig. 2 shows the sensing probability distribution of the target point p ($R_s = 10$, $r_e = 2.5$).

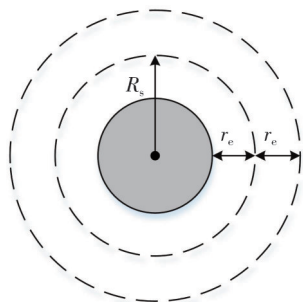


Fig. 1 Sensing model

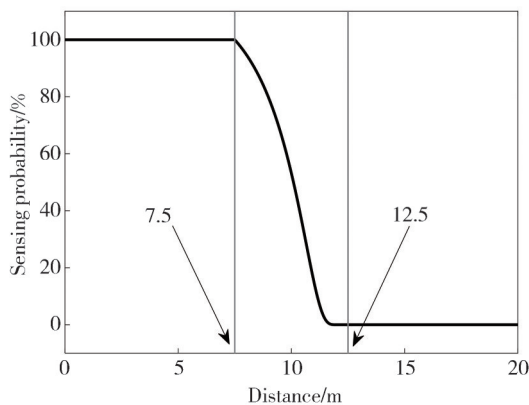


Fig. 2 Sensing probability distribution

In the monitoring area, if the target point p can be sensed by any node in the node set $S = \{S_1, S_2, \dots, S_N\}$, the target point p is covered by the network. The joint sensing probability of point p is C_p , and the calculation method is shown as

$$C_{p, \text{all}} = \begin{cases} 1, & 1 - \prod_{i=1}^N (1 - C_{p,i}) \geq C_{\text{th}}, \\ 0, & 1 - \prod_{i=1}^N (1 - C_{p,i}) < C_{\text{th}}, \end{cases} \quad (3)$$

where $C_{\text{th}} = 0.8$ is the minimum joint sensing probability when the target point is covered, and N is the total number of nodes.

1.1 Network coverage rate

The network coverage rate R is an important indicator to evaluate the network coverage. It is the ratio of the size of coverage area to the size of the whole network area^[15]. The calculation method of R is shown as

$$R = \frac{\sum_{X_p=1}^N \sum_{Y_p=1}^N C_{p, \text{all}}}{N \times N}. \quad (4)$$

1.2 Coverage uniformity

The coverage uniformity U of the network is used to evaluate the distribution of nodes in the network, which is equal to the average of the standard deviation of the distance between all nodes in the network and its neighbor nodes, with a smaller uniformity indicating a more uniform distribution of nodes^[16]. The calculation method of U is shown as

$$U = \frac{1}{N} \sum_{i=1}^N U_i, \quad (5)$$

$$U_i = \sqrt{\frac{1}{k_i} \sum_{j=1}^{k_i} (d_{i,j} - d_{i, \text{avg}})^2}, \quad (6)$$

where U_i denotes the standard deviation of the distance between node S_i and its neighbor nodes; k_i denotes the number of neighbor nodes of node S_i ; $d_{i,j}$ denotes the distance between node S_i and node S_j ; and $d_{i, \text{avg}}$ denotes the average distance between node S_i and its neighbor nodes.

2 Virtual force node deployment method based on Voronoi diagram

The virtual force algorithm guides the nodes to update its position through total forces on the nodes to find the optimal deployment position of the nodes. The forces on the nodes include the virtual forces between the nodes, the virtual forces on the nodes from boundaries or obstacles, and the virtual forces on the nodes from the centre of the Thiessen polygon where the nodes are located.

2.1 Virtual force on the node

2.1.1 Virtual force between nodes

Definition: Node visibility.

If the connection between two nodes does not pass through an obstacle, it is said that the two nodes are visible. As shown in Fig.3, the connection between node S_1 and node S_2 does not pass through obstacles, the connection between S_1 and node S_3 and the connection between S_2 and node S_3 have passed the obstacle, therefore, node S_1 and node S_2 are visible, node S_3 does not visible with nodes S_1 and S_2 .

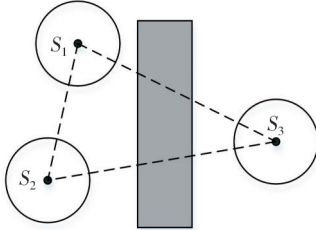


Fig. 3 Node visibility diagram

In the network, only the nodes that are visible can generate virtual force. Assuming that node S_i and node S_j are visible, the calculation method of the virtual force F_{ij} of node S_j on node S_i is shown as

$$F_{i,j} = \begin{cases} 0, & d_{i,j} > R_c, \\ (\omega_a(d_{i,j} - d_{th}), \alpha_{i,j}), & R_c \geq d_{i,j} > d_{th}, \\ 0, & d_{i,j} = d_{th}, \\ (\omega_b(d_{th} - d_{i,j}), \alpha_{i,j} + \pi), & d_{i,j} < d_{th}, \end{cases} \quad (7)$$

where $d_{i,j}$ denotes the distance between node S_i and node S_j ; $\alpha_{i,j}$ denotes the direction angle of the line segment connecting node S_i and node S_j ; ω_a and ω_b denote the virtual force gravitational and repulsive coefficients, respectively; d_{th} denotes the distance threshold between nodes; R_c denotes the communication radius of the node. If $d_{i,j}$ is less than d_{th} , the node is subjected to repulsive force, and if $d_{i,j}$ is greater than d_{th} and less than or equal to R_c , the node is subjected to gravitational force.

2.1.2 Virtual force exerted on the node by area boundary or obstacle

The calculation method of the virtual force $F_{i,b}$ of the area boundary or obstacle on the node S_i is shown as

$$F_{i,b} = \begin{cases} 0, & d_{i,b} > R_c, \\ (\omega_a(d_{i,b} - d_{b,th}), \alpha_{i,b}), & R_c \geq d_{i,b} > d_{b,th}, \\ 0, & d_{i,b} = d_{b,th}, \\ (\omega_b(d_{b,th} - d_{i,b}), \alpha_{i,b} + \pi), & d_{i,b} < d_{b,th}, \end{cases} \quad (8)$$

where $d_{i,b}$ denotes the distance between node S_i and the area boundary or obstacle; $d_{b,th}$ is the safe distance between the node and the area boundary or obstacle, $d_{b,th} = d_{th}/2$. If $d_{i,b}$ is greater than $d_{b,th}$ and less than or equal to R_c , the node will be subjected to gravitational

force; and if $d_{i,b}$ is less than $d_{b,th}$, the node will be subjected to repulsive force.

2.1.3 Virtual force exerted on the node by centroid of Thiessen polygon

The Voronoi diagram consists of a set of polygons which is composed of vertical bisectors of connecting straight lines at two adjacent points. When constructing Voronoi diagram, firstly, the nodes in the monitoring area are Delaunay triangulated to form a Delaunay triangulation network, and then the vertical bisector of each Delaunay triangle edge is made. The convex polygons composed of vertical bisectors are called Thiessen polygons, and diagram composed of Thiessen polygons are called Voronoi diagrams. The Voronoi diagram is built as shown in Fig.4.

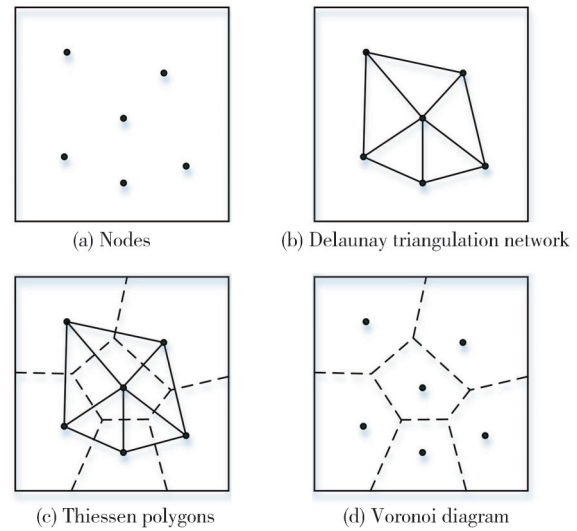


Fig. 4 Construction process of a Voronoi diagram

After the Voronoi diagram is built in the monitoring area, every node has its own corresponding Thiessen polygon. As shown in Fig.5, where “•” represents the position of the node, and “+” represents the position of the centroid of Thiessen polygon. When the monitoring area is evenly covered by the nodes, the area of each Thiessen polygon should be the same. Therefore, we divide node into two cases according to the size of the area of the Thiessen polygon it belongs to.

Case 1: The area of the Thiessen polygon to which the node belongs is larger than the average area of the Thiessen polygon.

In this case, the redundant coverage area between the node and other nodes is small, the distance between nodes is far, and the virtual force is small. If only relying on the virtual force between the nodes and the virtual force of the boundary and obstacles on the node to guide the movement of the node, the nodes move smaller distance and the algorithm convergence speed is slow.

Therefore, it is also necessary to consider the virtual force exerted on the node by the centroid of the Thiessen polygon and guide the node to update its position through total force. As shown in Fig.5, the area of the Thiessen polygon where S_1, S_4, S_5 and S_9 are located is larger than the average area. It is necessary to calculate the virtual force between the nodes, the virtual force of the boundary and obstacles on the nodes, and the virtual force of the centroid of the Thiessen polygon on the node. The node position is updated by the total force of these virtual forces.

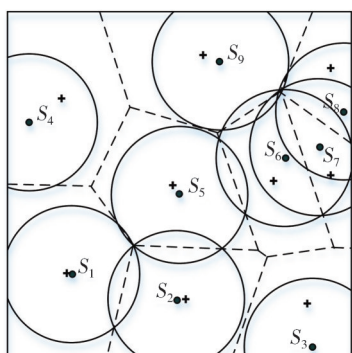


Fig. 5 Voronoi diagram of monitoring area

Case 2: The area of the Thiessen polygon to which the node belongs is smaller than the average area of the Thiessen polygon.

In this case, the redundant coverage area between nodes is large, the distance is close, and the virtual force is obvious. Only relying on the virtual force between the nodes and the virtual force of the boundary and obstacles on the nodes to guide the movement of the nodes, the nodes may quickly disperse. Therefore, when the area of the Thiessen polygon to which the node belongs is less than the average area, such as nodes $S_6, S_7,$ and S_8 in Fig. 5, only the virtual forces between nodes and the virtual forces of the boundary and obstacles to node need to be considered to update its positions.

For the centroid of Thiessen polygon, assuming that the coordinates of the vertices of Thiessen polygon at which node S_i is located are $(X_1, Y_1), (X_2, Y_2), \dots, (X_k, Y_k)$, the calculation method of the centroid coordinates (C_x, C_y) of the Thiessen polygon at which node S_i is located is shown as^[17]

$$C_x = \frac{\frac{1}{6} \sum_{i=1}^k (X_i + X_{i+1})(X_i + Y_{i+1} - X_{i+1} + Y_i)}{M}, \quad (9)$$

$$C_y = \frac{\frac{1}{6} \sum_{i=1}^k (Y_i + Y_{i+1})(X_i + Y_{i+1} - X_{i+1} + Y_i)}{M}. \quad (10)$$

The calculation method of the virtual force $F_{i,c}$ that the

centroid of Thiessen polygon on the node is

$$F_{i,c} = \begin{cases} \omega_a \times d_{i,c} \alpha_{i,c}, & A_i > A_{avg}, \\ 0, & A_i \leq A_{avg}, \end{cases} \quad (11)$$

where $d_{i,c}$ denotes the distance from node S_i to the centroid of Thiessen polygon, A_i denotes the area of the Thiessen polygon at which node S_i is located, and A_{avg} denotes the average area of the Thiessen polygon. Only when the area of the Thiessen polygon to which node S_i belongs is larger than the average area, node S_i will be subjected to the virtual force of the centroid of the Thiessen polygon.

2.1.4 Virtual resultant force on the node

The calculation method of the total force on the node S_i is

$$F_i = \sum_{j=1, j \neq i}^k F_{i,j} + F_{i,b} + F_{i,c}, \quad (12)$$

where k denotes that a total of k nodes in the network exert a virtual force on node i . After calculating the total force of node i , the node will move from its original position $(X_{i,old}, Y_{i,old})$ to a new position $(X_{i,new}, Y_{i,new})$ under the action of the total force F_i . The calculation methods of $X_{i,new}$ and $Y_{i,new}$ are respectively shown as

$$X_{i,new} = X_{i,old} + \frac{F_x}{F} \times D, \quad (13)$$

$$Y_{i,new} = Y_{i,old} + \frac{F_y}{F} \times D, \quad (14)$$

where F_x and F_y are the component forces of the total force in the x -axis direction and the y -axis direction, respectively; F is the maximum repulsive force between the two nodes, $F = \omega_b \times d_{th}$; and D is the unit step size of the node movement. In the early stage of the algorithm, the total force exerted on the node is larger and the moving distance is long. In the late stage of the algorithm, the total force exerted on the node is smaller and the moving distance is small. This can speed up the convergence speed of the algorithm, and alleviate the phenomenon of oscillations.

2.1.5 Out-of-bounds handling

During the operation of the algorithm, the node updates its position according to the total force on it, it will encounter the following two special situations.

Case 1: The node is outside the monitoring area after updating its position according to the total force.

For node S_1 in Fig. 6, $S_{1,old}$ is the position of node S_1 before updating its position, and S_1 is outside the monitoring area after updating its position, therefore, the position of the node needs to be corrected. The method in this work is to make a line segment

perpendicular to the boundary with the node as the end point, and the line segments on both sides of the boundary are of the same length, and the end of the line segment that lies within the monitoring area is the final position of the node.

Case 2: The node is inside the obstacle after updating its position according to the total force.

For node S_2 in Fig. 6, $S_{2,old}$ is the position of node S_2 before updating its position, and S_2 is inside the obstacle after updating its position. The method of correcting the position of the node is to make a line segment in the direction of the node movement, the length of the line segment is equal to the length of the line intercepted by the obstacle, and the other end of the line segment is the final position of the node.

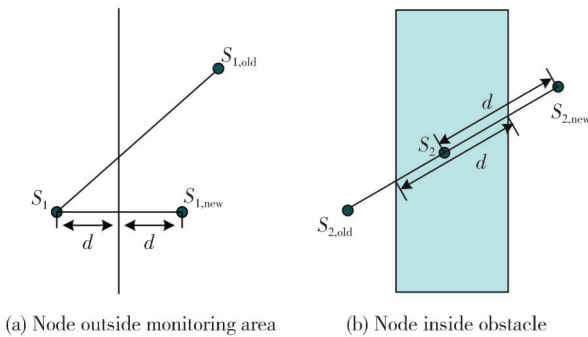


Fig. 6 Out-of-bounds handling diagram

2.2 Distance threshold

In the virtual force algorithm, the distance threshold can adjust the force properties between nodes. When using the Boolean sensing model, the distance threshold is only related to the sensing radius of the node. When using the probabilistic sensing model, the distance threshold should be calculated based on a series of parameters such as the sensing radius of the node and measurement reliability parameters. To reduce node coverage redundancy and avoid vulnerabilities in node coverage area, the nodes in this work use the deployment strategy shown in Fig. 7.

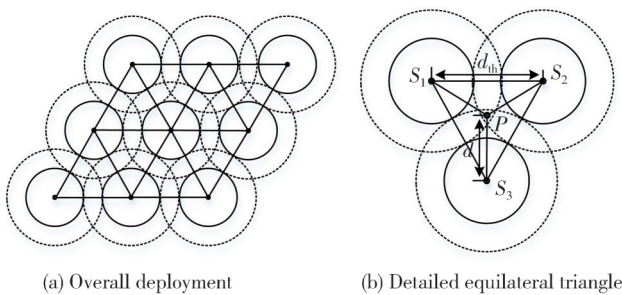


Fig. 7 Equilateral triangle deployment

As shown in Fig. 7, the connection of three adjacent nodes forms an equilateral triangle, and the central point

P of the equilateral triangle is the point with the smallest joint perception probability in this triangle. To avoid monitoring vulnerabilities in redundant coverage areas between nodes, the joint perception probability of point P should be equal to C_{th} .

$$1 - \left(1 - e^{(-\lambda_1 \alpha_1^{\beta_1} / \alpha_2^{\beta_2} + \lambda_2)} \right)^3 = C_{th}, \tag{15}$$

where $\alpha_1=r_e-R_s+d$, $\alpha_2=r_e+R_s+d$, $\lambda_1=1$, $\lambda_2=0$, $\beta_1=1$, $\beta_2=1.5$, the node perception radius is $R_s=10$, and the measured reliability parameter $r_e=2.5$. Substituting these parameters into the above formula, we can get $d \approx 10.32$ and the distance threshold between the nodes $d_{th} = 2 \times 10.32 \times \sin 60^\circ \approx 17.87$.

2.3 Steps of deployment method

Step 1 Deploy N nodes randomly in the monitoring area.

Step 2 Construct a Voronoi diagram in the monitoring area and determine the Thiessen polygon of each node.

Step 3 Calculate the total force on all nodes:

The virtual force between nodes (Eq. (7));

The virtual force of the area boundary or obstacle on the node (Eq. (8));

The virtual force exerted on the node by the centroid of the Thiessen polygon at which the node is located (Eq. (11));

The virtual resultant force on the node (Eq. (12)).

Step 4 Update the position of all nodes according to Eqs. (13) and (14).

Step 5 Repeat steps 2 – 4 until the stop condition is met.

3 Simulation and analysis

Matlab was used to simulate the proposed VFAVD algorithm via two ways—with obstacles and without obstacles in the monitoring area, and the algorithm is evaluated from the two aspects of network coverage rate and coverage uniformity. The relevant parameters of the simulation are listed in Table 1.

Table 1 Relevant parameters of simulation

Parameter	Value
Network area/(m × m)	100 × 100
N	35
T	500
ω_a	1
ω_b	1 000
C_{th}	0.8
R_s/m	10
r_e/m	2.5
d_{th}/m	17.87
D/m	1

3.1 No obstacles in monitoring area

Supposing the monitoring area is a two-dimensional plane area without obstacles, Fig.8 shows the final node deployment of five algorithms. Fig.8(a) shows the initial distribution of nodes with a coverage rate of 57%. The coverage rates of the VFA, IVFAB, BCBS, DV, and VFAVD algorithms are 75.89%, 87.98%, 85.93%, 88.55% and 90.65%, respectively. We can see that the VFAVD algorithm has a more uniform distribution of

nodes compared to the remaining four algorithms, and also has better coverage near the boundary of the monitoring area than the other algorithms. This is because the VFAVD algorithm considers the repulsive force of the boundary on the nodes to optimize the coverage near the boundary. Meanwhile, the global search capability of the algorithm is enhanced by calculating the force of the Thiessen polygon center on the nodes, which makes the nodes more uniformly distributed.

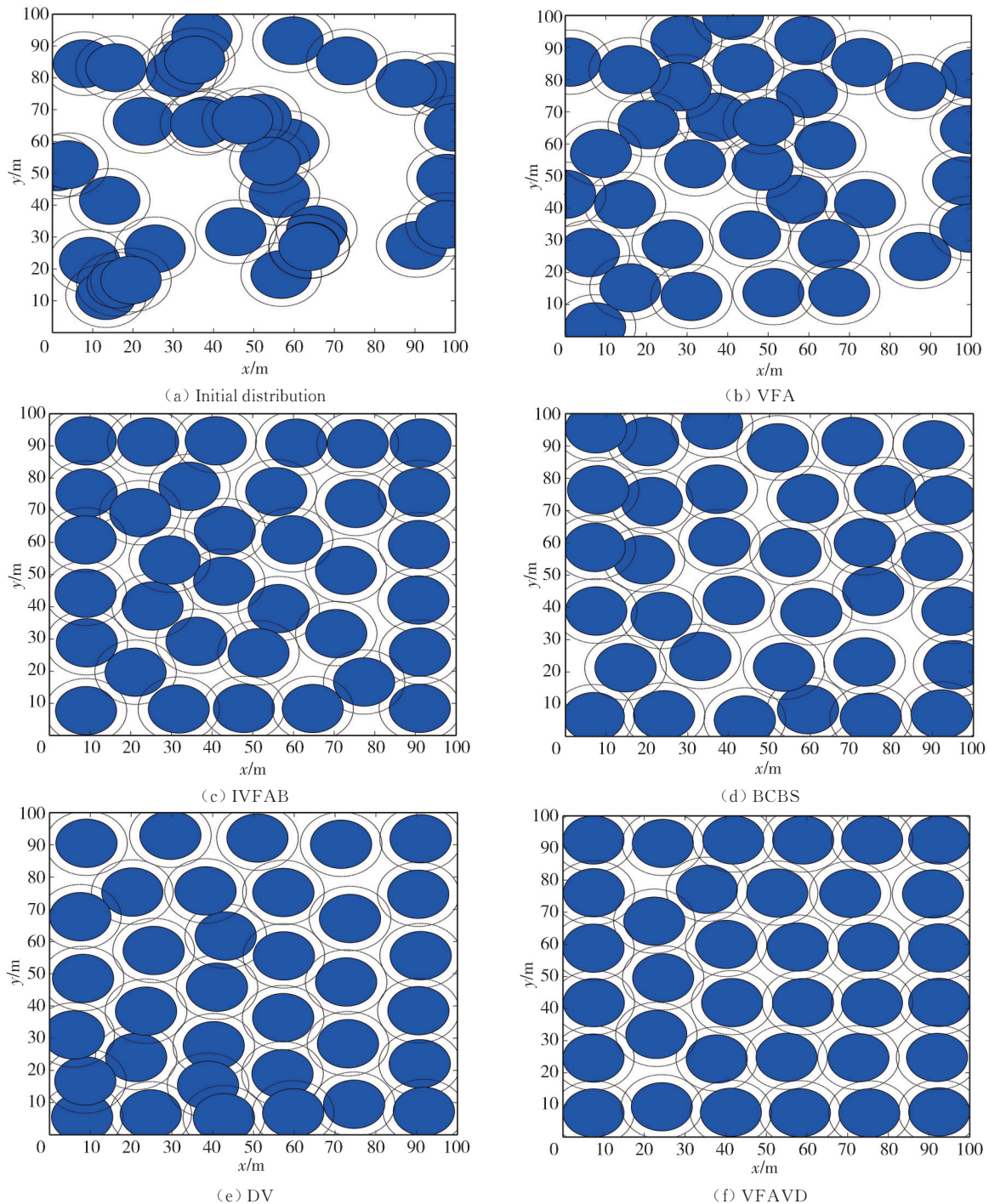


Fig. 8 Distribution of nodes

Fig. 9 shows the network coverage rates of the five algorithms varying with the number of iterations. In the first 100 iterations, the network coverage rates of VFAVD, IVFAB, and BCBS algorithms have improved significantly, while the network coverage rates of the DV and VFA algorithms have increased slowly. Among them, the VFAVD algorithm has the fastest convergence rate, and the final coverage rate is also greater than that of the other four algorithms.

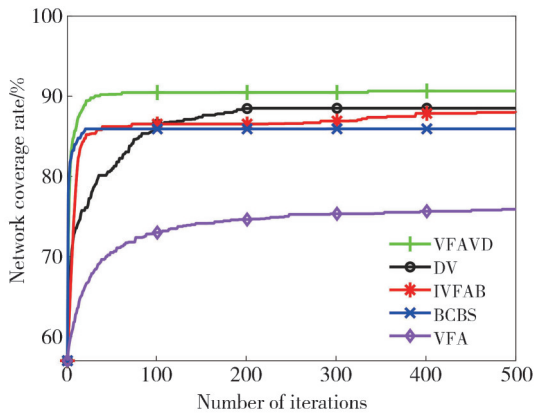


Fig. 9 Network coverage rate

Fig. 10 compares the coverage rates of the five algorithms as the number of nodes increases. We can see that as the number of nodes increases, the coverage rate of the five algorithms maintains an upward trend. When the number of nodes is 30, the advantage of VFAVD algorithm is not obvious due to the small number of nodes. However, as the number of nodes increases, the coverage of VFAVD algorithm continues to rise and is always higher than the other four algorithms. Fig. 11 shows the comparison of coverage uniformity with different number of nodes. We can see that the coverage uniformity of the VFAVD algorithm is much smaller than that of the BCBS, DV and IVFAB algorithms although the coverage rate is similar to that of these three

algorithms when the number of nodes is 30. This indicates that the nodes of the VFAVD algorithm are more evenly distributed. As the number of nodes increases, the coverage uniformity of the five algorithms continues to increase, but the coverage uniformity of the VFAVD algorithm is consistently smaller than that of the remaining four algorithms.

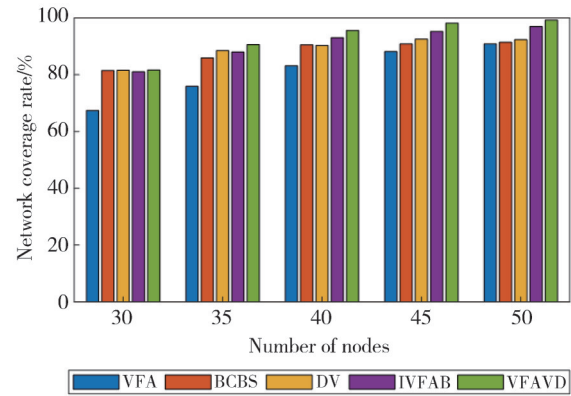


Fig. 10 Network coverage rate with different node numbers

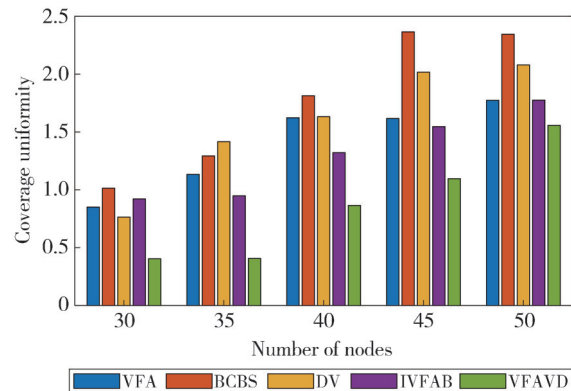
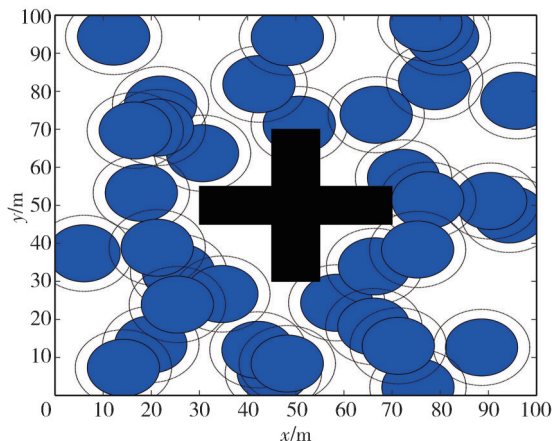


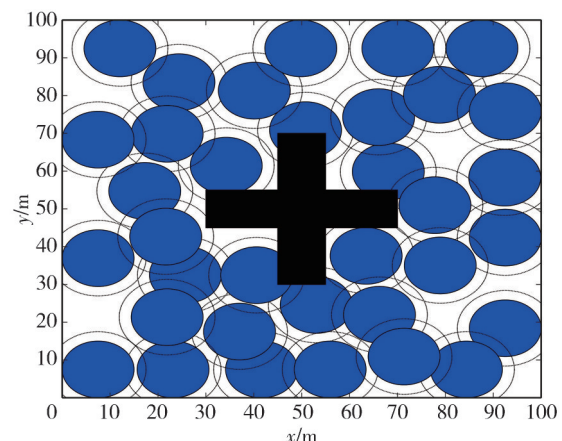
Fig. 11 Coverage uniformity with different number of nodes

3.2 With obstacles in monitoring area

Supposing the monitoring area is a two-dimensional plane area and there is a “+”-shaped obstacle in the area, Fig.12 shows the final node deployment of the five algorithms in the presence of obstacles.



(a) Initial distribution



(b) VFA

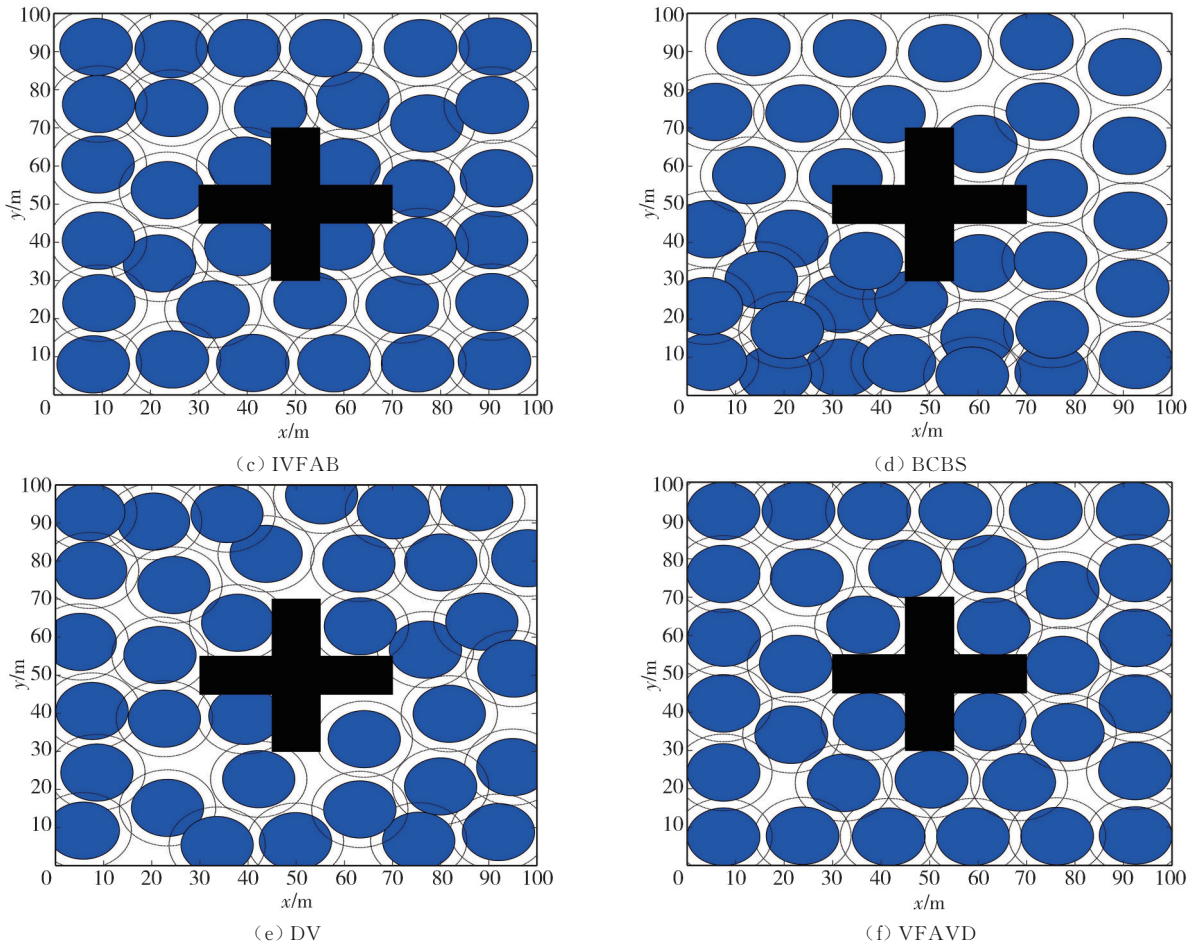


Fig. 12 Distribution of nodes

Fig. 12 (a) shows the initial distribution of nodes with a coverage rate of 68.17%. The coverage rates of the VFA, IVFAB, BCBS, DV, and VFAVD algorithms are 84.28%, 90.81%, 89.29%, 87.48% and 93.01%, respectively. We can see that the distributions of VFA, IVFAB, BCBS and DC algorithms around the obstacles are not good when there are obstacles in the region, and the BCBS algorithm even shows a non-uniform distribution of nodes. The VFAVD algorithm can effectively identify obstacles and provide better coverage around obstacles. At the same time, the coverage of the whole network is optimized by calculating the force of the Thiessen polygon center on the nodes, and the nodes are more uniformly distributed to avoid the phenomenon of non-uniform distribution of nodes.

Fig. 13 shows the network coverage rates varying with the number of iterations when there are obstacles in the monitoring area. Compared to the case without obstacles, the VFAVD, IVFAB and BCBS algorithms still maintain a fast convergence rate, the convergence rate of DV algorithm becomes slower at the beginning of the operation, and the convergence rate of the VFA algorithm does not change significantly. Among them, the VFAVD algorithm

has the fastest convergence rate, reaching the optimal deployment within the first 100 iterations, and the coverage rate is consistently higher than that of the remaining four algorithms. Fig. 14 and Fig. 15 show the variation of network coverage rate and coverage uniformity with increasing number of nodes for the five algorithms when there are obstacles in the monitoring area, respectively. We can see that when there are obstacles in the monitoring area, as the number of nodes increases, the VFAVD algorithm is still better than the other four algorithms in terms of network coverage rate and coverage uniformity.

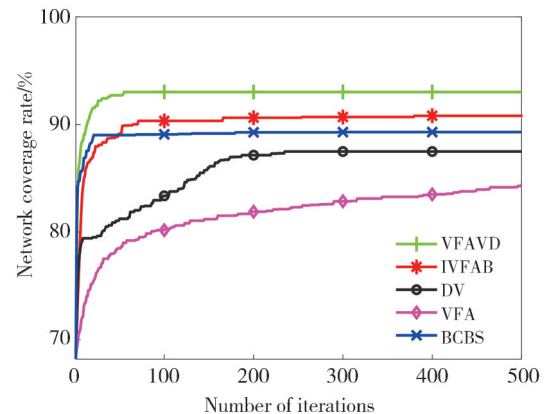


Fig. 13 Network coverage rate

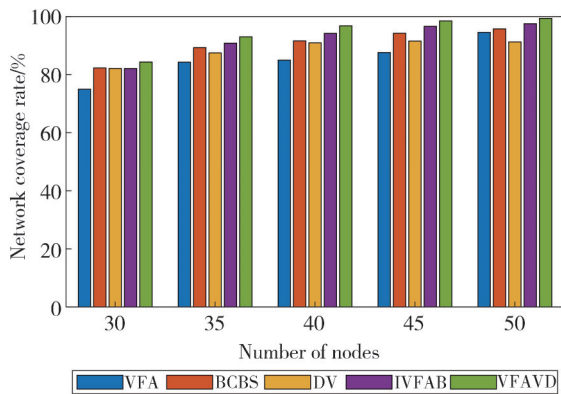


Fig. 14 Network coverage rate with different number of nodes

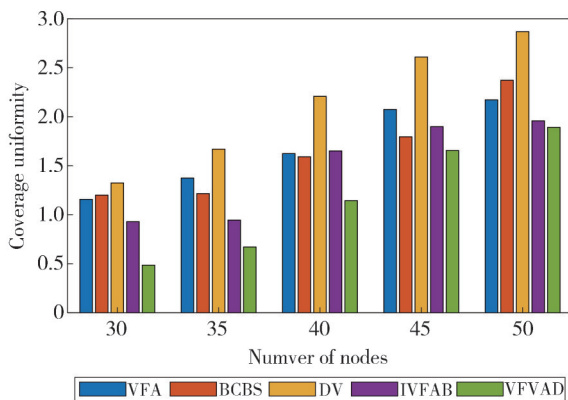


Fig. 15 Coverage uniformity with different number of nodes

4 Conclusions

Node deployment has an important impact on network performance. In terms of the node deployment of field observation instruments in cold and arid areas, we propose a virtual force node deployment algorithm based on Voronoi diagram. The algorithm adopts the probability sensing model, which is more in line with the actual situation. After constructing a Voronoi diagram in the monitoring area, the Thiessen polygon of each node is determined, and the global search capability of the algorithm is enhanced through the virtual force of the centroid of the Thiessen polygon on the node. In addition, we introduce the unit step size to accelerate the convergence speed of the algorithm. Compared with the existing algorithms, the proposed algorithm has better performance in terms of network coverage rate and coverage uniformity.

Acknowledgement

This work was supported by National Natural Science Foundation of China (No. 61862038), and Lanzhou Talent Innovation and Entrepreneurship Technology

Plan Project (No. 2019-RC-14).

Declaration of conflicting interests

The authors have no conflict of interests related to this publication.

References

- [1] HUO J Y, YANG J G, AL-NESHMI H M M. Design of layered and heterogeneous network routing algorithm for field observation instruments. *IEEE Access*, 2020, 8: 135866-135882.
- [2] HUO J Y, ZHANG Y N, LIU L Q. The research and design of network routing protocol for field observation instruments. *International Journal of Sensor Networks*, 2014, 16(2): 87.
- [3] LI M, HU J P, CAO X L. Minimum cost of node deployment strategy for heterogeneous sensor networks. *Journal of Xidian University*, 2021, 48(4): 11-19.
- [4] ZOU Y, CHAKRABARTY K. Sensor deployment and target localization in distributed sensor networks. *ACM Transactions on Embedded Computing Systems*, 2004, 3(1): 61-91.
- [5] TENG Z J, ZHANG L, GUO L W, et al. Intensity-based virtual force deployment algorithm with boundary forces. *Chinese Journal of Sensors and Actuators*, 2018, 31(7): 1072-1076.
- [6] LI C R, XIE J L, ZHANG C X, et al. Optimal node deployment in WSN based on virtual force. *Journal of the China Railway Society*, 2018, 40(9): 71-76.
- [7] ZHOU F, GUO H T, YANG Y. An improved virtual force relocation coverage enhancement algorithm. *Journal of Electronics and Information Technology*, 2020, 42(9): 2194-2200.
- [8] MAHBOUBI H, AGHDAM A G. Distributed deployment algorithms for coverage improvement in a network of wireless mobile sensors: relocation by virtual force. *IEEE Transactions on Control of Network Systems*, 2017, 4(4): 736-748.
- [9] FANG W, SONG X H. A deployment strategy for coverage control in wireless sensor networks based on the blind-zone of Voronoi diagram. *Acta Physica Sinica*, 2014, 63(22): 132-141.
- [10] TAN L, TANG X J, HUSSAIN A, et al. A weighted voronoi diagram-based self-deployment algorithm for heterogeneous directional mobile sensor networks in three-dimensional space. *IEICE Transactions on Communications*, 2020, 103(5): 545-558.
- [11] DING X, WU X B, HUANG C. Area coverage problem based on improved PSO algorithm and feature point set in wireless sensor networks. *Acta Electronica Sinica*, 2016, 44(4): 967-973.
- [12] JIN H L, LIU B T, CHEN W, et al. Research on the nodes deployment scheme for sensor coverage in underwater wireless networks based on genetic algorithm.

- Chinese Journal of Sensors and Actuators, 2019, 32(7): 1083-1087.
- [13] JIA J, CHEN J, CHANG G R, et al. Optimal coverage scheme based on genetic algorithm in wireless sensor networks. *Control and Decision*, 2007, 22(11): 1289-1292.
- [14] WANG S P. Research on coverage optimization algorithms for wireless sensor network. Changchun: Jilin University, 2020.
- [15] SUN Z Y, LI C F, XING X F, et al. Optimization cooperative coverage algorithm with controllable threshold-parameters in WSNs. *Journal of Frontiers of Computer Science and Technology*, 2021, 15(5): 893-906.
- [16] LIU W T, FAN Z Y. Coverage optimization of wireless sensor networks based on chaos particle swarm algorithm. *Journal of Computer Applications*, 2011, 31(2): 338-340.
- [17] YU Q, YUE D P, YANG D, et al. Layout optimization of ecological nodes based on BCBS model. *Transactions of the Chinese Society for Agricultural Machinery*, 2016, 47(12): 330-336.

基于 Voronoi 图的野外观测仪器虚拟力节点部署方法

火久元^{1,2,3*}, 王 磊¹

1. 兰州交通大学 电子与信息工程学院, 甘肃 兰州 730070;

2. 兰州华浩科技有限公司, 甘肃 兰州 730070;

3. 国家冰川冻土沙漠科学数据中心, 甘肃 兰州 730070

摘 要: 针对寒旱区野外观测仪器网络在监测区域的节点部署, 提出了一种基于 Voronoi 图的虚拟力节点部署算法 (Virtual force algorithm based on Voronoi diagram, VFAVD)。该方法采用了更加符合实际情况的概率感知模型。首先, 在监测区域构建 Voronoi 图, 以确定每个节点的泰森多边形。其次, 计算每个节点所受的虚拟作用力, 并根据虚拟合力的方向和大小更新节点的位置, 从而达到提高网络覆盖率的目的。仿真结果表明, VFAVD 算法能够有效提高网络的覆盖率, 并且在覆盖均匀度方面也有很好的效果。

关键词: 野外观测仪器网络; 节点部署; Voronoi 图; 虚拟力; 网络覆盖率

引用格式: HUO Jiuyuan, WANG Lei. Virtual force node deployment algorithm of field observation instrument based on voronoi diagram. *Journal of Measurement Science and Instrumentation*, 2025, 16(3): 435-445. DOI: 10.62756/jmsi.1674-8042.2025042